Journal of Scientific & Industrial Research
Vol. 81, January 2022, pp. 84-93

Design Optimization of a 4-Poled 1500 rpm 25 kVA SG to Obtain the Desired Magnetic Flux Density Distributions by using RSM

Aslan Deniz Karaoglan[1]* and Deniz Perin[2]
[1]Balikesir University, Balikesir 10 145, Turkey
[2]ISBIR Electric Company, Balikesir 10 150, Turkey

Received 18 February 2021; Revised 06 December 2021; Accepted 07 December 2021

In this study design optimization for 4-poled 1500 rpm 25 kVA synchronous generator (SG) is performed. The aim is to determine the optimum factor levels for the design parameters namely slot opening width (Bs0), height, and width to keep the responses namely 'pole-body flux density' and 'air-gap flux density' distributions in a desired range. The target values are determined as 1.75 Tesla and 0.9 Tesla for the 'pole-body flux density' and 'air-gap flux density' respectively. For this purpose, Response Surface Methodology (RSM) is used for optimization. Numerical simulations are performed in the Maxwell environment and the optimization by RSM is performed by Minitab statistical package. Desired goals were achieved and optimum factor levels were determined with RSM. Then the results of RSM are compared by Genetic Algorithm (GA), Particle Swarm Optimization algorithm (PSO), and Modified Social Group Optimization (MSGO) algorithm. These methods are evaluated together in terms of advantages and disadvantages. The comparisons indicate that using RSM provides acceptable results without performing coding effort and also provides users to understand the relations visually between the factors and the responses by the aid of 'Minitab Response Optimizer Module'.

Keywords: Electric machine design, Genetic algorithm, Regression, Response surface methodology, Synchronous generator

Introduction

Synchronous Generator (SG) design optimization is investigated by many researchers. In these studies, Total Harmonic Distortion (THD), efficiency, magnetic flux density distribution and etc. are widely selected performance criteria those are tried to be improved. Magnetic flux density distribution is an important performance criterion which must be kept in a particular range to provide the high efficiency for the electric machine. For the design optimization many different methods are used. Because of having so many design combinations, it is impossible to perform the optimization by using the real experimental results. Instead of this, simulation results are widely used. The related remarkable studies about the SG design optimization are as follows. Gizolme *et al.* studied on the pole shape optimization of SG rotor. They used 2D Finite Element Analysis (FEA) and Genetic Algorithm (GA) together to minimize the flux density harmonics.[1] Gillon & Brochet have been researching the optimization of the design of an electric motor using RSM. As design parameters for optimization, they used half tooth, yoke thickness, slot height, open angular tooth, tooth head thickness, magnet thickness, air-gap, open angular magnet, and radius shaft.[2] Jolly *et al.* used RSM and GA to optimize Permanent Magnet Motor (PMM) design parameters and they used FEA for numerical experiments. Torque and speed are chosen as the variables that influence the responses.[3] Fang *et al.* studied on Interior PM Synchronous Motors (IPMSM). Using RSM, the optimal configuration of the double-layer IPMSM model is effectively calculated. Numerical experiments are performed using equivalent circuit method and FEA. Design parameters those have to be optimized are selected as; lengths of 1st & 2nd PM layers, break angles of 1st & 2nd PM segments.[4] Hasanien & Muyeen performed optimization by using GA and RSM to optimize the PI parameters of Variable Speed Wind Turbine (VSWT) driven PMSG's frequency converter. The responses are considered as the settling time, the maximum percentages undershoot - overshoot, and steady—state error of the voltage profile.[5] Zhang *et al.* suggested a method to optimize a transverse flux PMM by using the Particle Swarm Optimization (PSO) algorithm and RSM together to maximize the no-load Electromotive Force (EMF).[6] Chai *et al.* performed rotor design

*Author for Correspondence
E-mail: deniz@balikesir.edu.tr

optimization of a PM wound field SG to maximize the average output torque and to decrease the torque ripple. They used 2D FEA, Kriging method and GA together.[7] Islam *et al.* optimized the design parameters namely slot wedge and semi-closed stator. They used 2D FEA and focused on air-gap flux density.[8] Soleimani *et al.* used RSM for optimizing high power Transverse Flux PM (TFPM) generators. The factors namely PM thickness, air-gap length, outer rotor radius, overlap between rotor length and PM are optimized.[9] Karaoglan *et al.* proposed RSM for optimizing the design parameters of stator slot of PMG.[10] They used Bs0, Bs1, Bs2, Hs2 parameters to optimize the responses namely: air-gap flux density, efficiency, statoryoke flux density and stator teeth flux density.

Optimizing the magnetic flux density distribution is investigated in several studies. In this paper, the goal is to find the optimum design values for some of the 4-pole 1500 rpm 25 kVA SG design parameters (slot opening width (Bs0), height and width) using RSM. In the electric engineering society literature, GA and PSO are the widely used optimization algorithms for design optimization. Modified Social Group Optimization (MSGO) which is the recently presented effective optimization algorithm is not previously used in this type of electric machine design optimization problem. So the findings are also compared to the results of GA, PSO, and MSGO optimization results. Optimum values for these design parameter combination together are not previously investigated for multi-objective optimization. Also the performance of RSM is not previously compared with GA, PSO, and MSGO for this type of problem. These are the novelty aspects of this research.

The motivation is to show the reader by visually the effect of these 3 design parameters on the magnetic flux by using minimum number of experimental runs. This study is performed in a real industrial plant and by considering only this limited number of parameters, we aimed to less affect the serial production line layout and its operations (such as the redesign of the assembly parts that may affect the standard production, body design, cooling design and etc.). Because of this reason the parameters (slot opening width (Bs0), height and width) those less affect the outer dimensions of the alternator is selected as the factors. Next section describes the details of the optimization method used in this study.

Materials and Methods

Since the RSM is first introduced in 1951, it became a commonly used Design of Experiment (DOE) approach used to model, analyze, and optimize processes with a minimum experimental runs. We used RSM — the synthesis of statistical and mathematical methods — to construct comprehensive mathematical models of complex systems that include several interaction parameters. RSM's key concept is to use a series of planned experiments at the first level with minimum runs. In the second step, regression modelling is conducted to achieve an optimal response by using these experimental findings. Finally in the third stage — to estimate the optimal solution-gradient search algorithm is used.[11–13] The goal of this paper is to optimize the slot opening width (Bs0), height, and width while keeping the responses namely 'pole-body flux density' and 'air-gap flux density' distributions in a desired range. In the first stage an experimental design is conducted by using orthogonal arrays and the responses are measured for each experimental run. Second stage of RSM is the modeling phase. Mathematical relationship between these factors and the responses must be determined. This is performed by using regression modeling. Regression models can be composed of linear terms, quadratic terms, and interaction terms. If a model has these three terms together then this model is called full quadratic model. The general representation of the model is given in Eq. (1).[11–13] This model will be calculated from the experimental runs obtained from the Maxwell simulations (given in the following section).

$$Y_i = \beta_0 + \sum_{k=1}^{m} \beta_k X_{ki} + \sum_{k=1}^{m} \beta_{kk} X_{ki}^2 + \sum_{k<l}^{m} \beta_{kl} X_{ki} X_{li} + e_i \quad \ldots(1)$$

$$\boldsymbol{\beta}^{\mathrm{T}} = [\beta_0, \beta_1, \beta_2, \ldots, \beta_m] \quad \ldots(2)$$

Y_i represents the response value for ith experimental run. In this study, there are 2 responses which mean that we will calculate 2 different regression equations in the next section. X terms are the values of the factors (in this study the factors are: X_1: slot opening width (Bs0), X_2: height, and X_3 : width). $X_{ki}X_{li}$ terms represents the interaction terms in the model (in this study there can be maximum 3 interaction terms such as $X_1 X_2$, $X_1 X_3$, $X_2 X_3$). e_i is the residual error for the i^{th} experimental run. $\boldsymbol{\beta}$ vector that is given in Eq. (2) includes the

coefficients of the models given in Eq. (1) and calculated as given below.[11–13]

$$\beta = (X^T X)^{-1}(X^T Y) \quad \ldots(3)$$

Y is called the response and represented by a column vector that is composed of the observed magnetic flux values from the Maxwell simulations. **X** represents the input matrix and composed of the runs performed in the experimental design for different combinations of the design parameters. The 1st column of X matrix is composed of 1s for the constant term (β_0) of the model. In a model that contains 3 factors; the 2nd, 3rd, and the 4th columns includes the factor values of X_1, X_2, and X_3 respectively. In this study 15 runs are designed for the experiments. These 3 columns (2nd, 3rd, and the 4th columns) and 15 rows are exactly the same as the experimental design. The 5th, 6th, and 7th columns of X matrix are composed of the squares of X_1, X_2, and X_3 respectively. The same issue is valid for the interactions. The interactions ($X_1 X_2$, $X_1 X_3$, $X_2 X_3$) are placed in the 8th, 9th, and 10th columns of X matrix by multiplying the related columns of X_1, X_2, and X_3. In other words in order to have columns containing all terms in the model, the **X** matrix is ordered.[11–13] When the data given in the following section are examined, it will be seen that for the regression model of pole-body flux density, the X matrix with dimensions of 15x10 will be obtained for 15 runs and 10 model coefficients (β). Similarly, for the regression model of air-gap flux density we will need another similar **X** matrix with same dimensions. R^2 (coefficient of determination) is determined after mathematical modeling to decide if the factors that are used in the mathematical model are sufficient to explain the change in response. In other words, R^2 represents the explanatory level between the model of regression and the factors.

$$R^2 = \frac{\beta^T X^T Y - n\overline{Y}^2}{Y^T Y - n\overline{Y}^2} \quad \ldots(4)$$

R^2 must be closer to 1 (which means 100 percent) in order to use the mathematical model, which is determined by the formulas given in Eqs (1–3), in the optimization stage. Since it implies in this situation that the variables used in modeling are adequate to describe the Y shift and there is no need to add additional variables to the model. If the R^2 is closer to 1, then the model's significance must be calculated in the last step prior to optimization. "Analysis of variance (ANOVA)" is used to do this. ANOVA is a statistical hypothesis test that utilizes the F-test to determine whether or not the regression model is significant. ANOVA has two hypotheses (H_0, H_1). H_0 implies the regression model is insignificant, while H_1 implies that the regression model is significant. So, H_1 must be valid in order to use the regression model in the optimization process. For hypothesis testing, the "p-value" technique may be used. In this analysis, Minitab's statistical package calculates the p-value. If the p-value is lower than the alpha (type-I error), it implies that H_1 is true and that the model is significant. The confidence level is selected as 95% in this study. This means the type-I error = α = 0.05 (5%). RSM can perform optimization using the gradient search algorithm if the model is significant. For GA optimization, these regression equations will also be used (for performing comparisons with RSM results).

Experimental Results and Discussions

In this study we used 4-poled 1500 rpm 25 kVA SG. The design of this SG is performed in Maxwell environment and values of the design parameters for this SG are listed in Table 1. The structure of the SG is also presented in Fig. 1. The SG is designed with 0.8 rated power factor. In the Maxwell design, all winding material is used as standard copper. Si—Fe is used for lamination. Finally H-Class insulation material is selected.

Table 1 — General design parameters for 4—poled 1500 rpm 25 k

Name	Value	Unit	Part	Description
Machine type	—	—	—	Three phase SG
Outer diameter	290	mm	Stator	Core dia. (yoke side)
Inner diameter	196.6	mm	Stator	Core dia. (gap side)
Skew width	1	Units	Stator	Slot range number
Length	170	mm	Stator	Core length
Slot type	3	N/A	Stator	Circular
Slots	36	Units	Stator	Number of slots
Hs0	1	mm	Stator	Slot opening height
Bs1	11.2	mm	Stator	Tooth width
Hs2	13.4	mm	Stator	Slot height
Outer diameter	195.4	mm	Rotor	Core dia. (yoke side)
Inner diameter	55	mm	Rotor	Core dia. (gap side)
Poles	4	—	Rotor	Number of poles
Length	170	mm	Rotor	Core length
Embrace	0.95	—	Rotor	Pole embrace

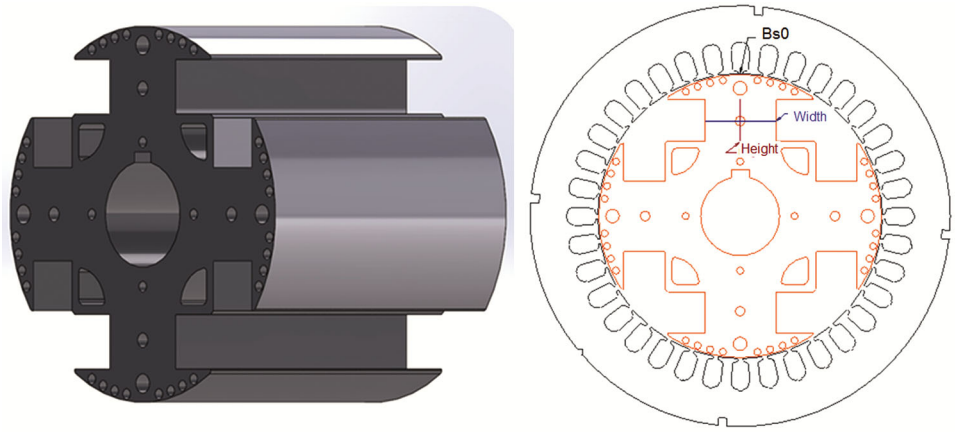

Fig. 1 — Structure of the SG

In the first stage the aim is to determine the mathematical relation between the factors (slot opening with (Bs0), height, and width) and the responses (pole-body flux density and air-gap flux density) by using regression modeling. To perform this phase, an experiment is designed by using 'RSM face centered design'. Table 2 presents the factor levels for this experimental design. The graphical presentation of the experimental design is given in Fig. 2. In the standard design the level-2 for width is 44.25 mm. However because of the constraints of serial production line, we used 44 mm instead of 44.25 mm in the experimental design.

Fifteen experimental runs are performed by Maxwell simulations, and the results are given in Table 3. By this way the drawback of producing real SG prototypes which is uncertain because of the costs is eliminated.

Calculations for regression modeling and the tests for model significance are performed by Minitab which is a well-known statistical package program. The mathematical models are given in Eqs. (5) & (6).

$$Y_1 = 4.915151518 - 0.005316826X_1 + 0.000933495X_2 - 0.111799819X_3 + 0.001615556X_1^2 - 0.000006007X_2^2 + 0.000845729X_3^2 + 0.000054375X_1X_2 - 0.000043790X_1X_3 - 0.000008033X_2X_3 \quad \ldots(5)$$

$$Y_2 = 0.935042990 - 0.009627237X_1 - 0.000089240X_2 - 0.000233876X_3 + 0.000108X_1^2 + 0.000001687X_2^2 + 0.000001659X_3^2 - 0.00000325X_1X_2 + 0.000022191X_1X_3 + 0.000000378X_2X_3 \quad \ldots(6)$$

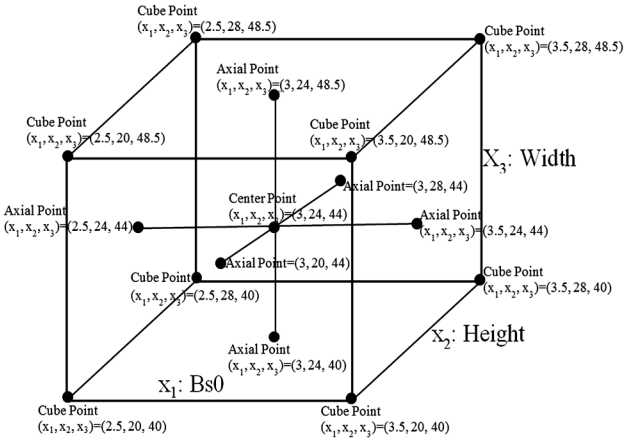

Fig. 2 — RSM face centered design

Table 2 — Factor levels that will be optimized

Factors	Symbols	Unit	Levels		
			1	2	3
Slot opening width (Bs0)	X_1	mm	2.5	3	3.5
Height	X_2	mm	20	24	28
Width	X_3	mm	40	44	48.5

The R^2 statistics associated with the regression models of models Y_1 and Y_2 are 100 and 99.99% respectively. The model significance is tested with ANOVA. P-value is calculated as 0.000 for both models (which is < 0.05). This means the models given in Eqs. (5) & (6) are significant and these models will be able to use for optimization. The RSM face-centered design appears to reflect the given set of design parameters with good precision. In Table 4, the model performances are presented. According to this Table, the results of Minitab are the predicted results

($\hat{Y}_i$), while the results of the Maxwell simulations are the observed responses (Y_i). PE (%) is the 'prediction error percentage". The formula given in Eq. (7) calculates PE (%):

$$PE_i(\%) = \frac{|Y_i - \hat{Y}_i|}{\hat{Y}_i} 100 \quad \ldots(7)$$

Results provided in Table 4 show that the regression models fit best with a maximum PE (%) < 0.03% in the given observations. Confirmation results are provided in Table 5.

Table 3 — The experimental design and simulation results

Run i	Factors			Responses	
				Pole-Body Flux Density (Tesla)	Air-Gap Flux Density (Tesla)
	X_{i1}	X_{i2}	X_{i3}	Y_{i1}	Y_{i2}
1	2.5	20	40.0	1.801	0.906
2	3.5	20	40.0	1.805	0.898
3	2.5	28	40.0	1.805	0.906
4	3.5	28	40.0	1.809	0.898
5	2.5	20	48.5	1.485	0.906
6	3.5	20	48.5	1.488	0.898
7	2.5	28	48.5	1.488	0.906
8	3.5	28	48.5	1.492	0.898
9	2.5	24	44.0	1.639	0.906
10	3.5	24	44.0	1.643	0.898
11	3.0	20	44.0	1.639	0.902
12	3.0	28	44.0	1.642	0.902
13	3.0	24	40.0	1.805	0.902
14	3.0	24	48.5	1.488	0.902
15	3.0	24	44.0	1.640	0.902

Table 4 — Regression model performances

Run(i)	Pole-Body Flux (Tesla)			Air-Gap Flux Density (Tesla)		
	Y_{i1}	$\hat{Y}_{i1}$	PE_{i1} (%)	Y_{i2}	$\hat{Y}_{i2}$	PE_{i2} (%)
1	1.801	1.80131	0.013	0.906	0.90620	0.002
2	1.805	1.80502	0.001	0.898	0.89804	0.001
3	1.805	1.80499	0.012	0.906	0.90619	0.003
4	1.809	1.80914	0.008	0.898	0.89801	0.001
5	1.485	1.48492	0.006	0.906	0.90599	0.001
6	1.488	1.48826	0.017	0.898	0.89803	0.003
7	1.488	1.48805	0.003	0.906	0.90601	0.001
8	1.492	1.49182	0.012	0.898	0.89802	0.002
9	1.639	1.63900	0.000	0.906	0.90605	0.005
10	1.643	1.64276	0.015	0.898	0.89796	0.004
11	1.639	1.63856	0.027	0.902	0.90201	0.001
12	1.642	1.64220	0.012	0.902	0.90200	0.000
13	1.805	1.80481	0.011	0.902	0.90205	0.006
14	1.488	1.48795	0.003	0.902	0.90196	0.005
15	1.640	1.64048	0.029	0.902	0.90198	0.002

The given observations in Table 5 are not used at the modeling phase previously. The findings provided in Table 5 show that the regression models have a reasonable good prediction performance (maximum PE (%) < 0.08%). Comparisons between the predicted values (Minitab results) and the observed values (Maxwell simulation results) have shown that it is possible to consider these numerical models for optimization. The 'Minitab Response Optimizer Module' is used to optimize the SG's design parameters for this purpose. The target values for the pole-body flux density and air-gap flux density are determined as 1.75 Tesla and 0.9 Tesla, respectively. In order for the system to reach high efficiency, it is necessary to reach the saturation of the sheet material used. The saturation point for 0.5 mm thick M530-50A sheet used in this study is given as 1.75 Tesla.[14] The value in the gap between the rotor and the stator, which has been saturated, was determined as 0.9 Tesla. This value was chosen as 0.9 Tesla, in accordance with the values between [0.8–1] Tesla in similar studies in the literature.[15]

According to Fig. 3, this goals are seems to be reached. Bs0 has negative effect on air-gap flux

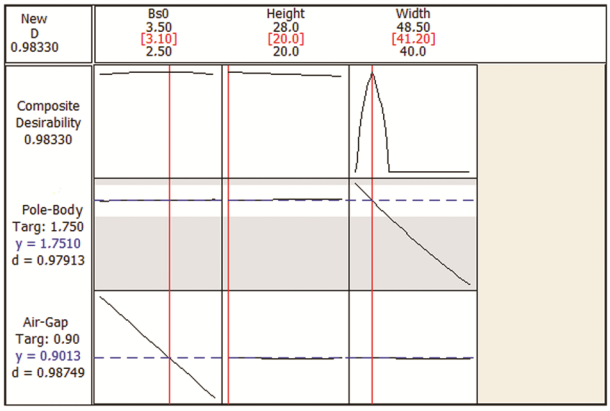

Fig. 3 — 'Minitab Response Optimizer'optimization results

Table 5 — Confirmation tests

Run	Factors			Pole-Body Flux Density (Tesla)			Air-Gap Flux Density (Tesla)		
	X_{i1}	X_{i2}	X_{i3}	Y_{i1}	$\hat{Y}_{i1}$	PE_{i1} (%)	Y_{i2}	$\hat{Y}_{i2}$	PE_{i2} (%)
16	2.7	22	42	1.716	1.71732	0.077	0.904	0.90447	0.052
17	2.7	22	46	1.567	1.56664	0.023	0.904	0.90439	0.043
18	2.7	26	42	1.719	1.71914	0.008	0.904	0.90446	0.051
19	2.7	26	46	1.569	1.56833	0.043	0.904	0.90439	0.043
20	3.3	22	42	1.719	1.71956	0.033	0.899	0.89959	0.066
21	3.3	22	46	1.569	1.56877	0.015	0.899	0.89957	0.063
22	3.3	26	42	1.721	1.72151	0.030	0.899	0.89958	0.065
23	3.3	26	46	1.571	1.57059	0.026	0.899	0.89956	0.063

Table 6 — Confirmations for the optimum factor levels of RSM

Response	Maxwell (for RSM results) (Y_i)	Minitab ($\hat{Y}_i$)	PE (%)	Maxwell (for GA results) (Y_i)	GA ($\hat{Y}_i$)	PE (%)	Maxwell (for PSO results) (Y_i)	PSO ($\hat{Y}_i$)	PE (%)	Maxwell (for MSGO results) (Y_i)	MSGO ($\hat{Y}_i$)	PE (%)
Pole-Body Flux Density (Tesla)	1.7585	1.7510	0.428	1.7585	1.7512	0.417	1.7580	1.7490	0.515	1.7580	1.7494	0.492
Air-Gap Flux Density (Tesla)	0.9030	0.9013	0.189	0.9045	0.9061	0.177	0.9025	0.8996	0.322	0.9025	0.8996	0.322

density (when the Bs0 increases the flux is decreasing), but it has no effect on pole-body flux density. The height has no significant effect on both responses. Finally, width has negative effect on pole-body flux density, but it has no effect on air-gap flux density. The optimum factor levels are calculated as Bs0: 3.1 mm, height: 20 mm, and width: 41.2 mm. Table 6 provides the observed Maxwell-simulated responses, the Minitab-fitted expected responses, and the PE. Results presented in this table indicate that, the maximum PE (%) < 0.5%. The pole-body flux density is calculated as 1.751 Tesla (with 0.428% PE) and air-gap flux density is calculated as 0.9013Tesla (with 0.189% PE). The harmonics of the optimized SG are measured as 0.89 (which is close to 0), according to Maxwell simulations. The magnetic flux distribution of optimized SG and the voltage graph are given in Figs. 4 and 5, respectively. Manufactured rotor of the optimized SG is given in Fig. 6.

In the electric engineering society, GA and PSO are widely used for optimization in the published papers. However the recently presented and effective MSGO is not used for this type of problem previously. So the optimization is also performed with these three optimization algorithm together and the results are compared with RSM. (The detail of the GA[16–18], PSO[19–21], and MSGO[22] can be referred from the papers presented in the references). Matlab program is used for coding GA, PSO, and MSGO. In order to use these equations in Matlab environment for multi-objective optimization, the models must be derived for coded factor levels between −1 and 1. By this way the models become independent from the units and the multi-objective optimization can be performed easily by summing all equations under a unique fitness function. The coding is performed by using Eq. (8). The regression models for coded factor levels are given in Eqs (9) and (10).

$$X_{coded} = \frac{X_{uncoded} - ((X_{max} + X_{min})/2)}{(X_{max} - X_{min})/2} \quad \ldots(8)$$

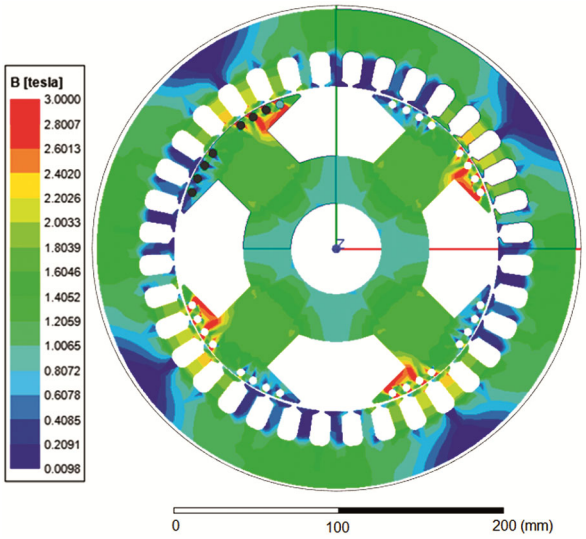

Fig. 4 — Magnetic flux density distribution of the optimized SG

$$Y_1 = 1.63111844135803 + 0.0018985131396957X_1 + 0.0017985822959891X_2 - 0.1584X_3 + 0.00038888888888935X_1^2 - 0.00011111111111121X_2^2 + 0.0152593364197531X_3^2 + 0.00012500000000016X_1X_2 - 0.00012638312586448X_1X_3 - 0.00012050484094056 9X_2X_3 \quad \ldots(9)$$

$$Y_2 = 0.902 - 0.004X_1 + 0.000000000000000000257647X_2 + 0.000000000000000000209257 6X_3 - 0.000000000000000000305262X_1^2 + 0.000000000000000000372999 9X_2^2 + 0.000000000000000000361943X_3^2 + 0.000000000000000000121491 3X_1X_2 - 0.000000000000000000557763 2X_1X_3 + 0.000000000000000000320851X_2X_3 \quad \ldots(10)$$

Haupt & Haupt[18] states that the continuous GA is faster than the binary GA, since before the cost function calculation, the chromosomes do not have to be decoded. Therefore, because of its benefit of having less storage, continuous GA was used in this study instead of binary GA. The maximum number of iterations in the algorithm is selected as 100000, with

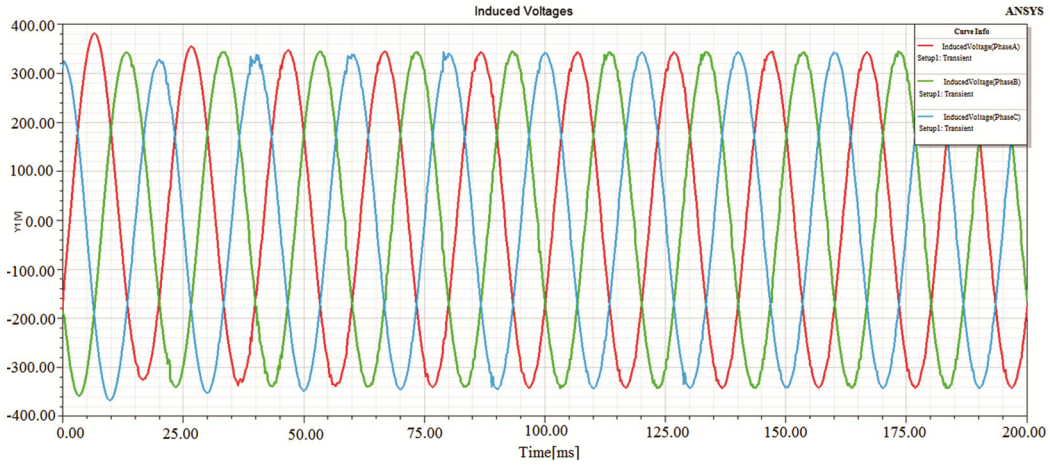

Fig. 5 — Voltage graph of the optimized SG

a population number of 8. The crossover and mutation rates are selected as 0.5 (50%) and 0.4 (40%), respectively. These GA parameters are tuned via a series of preliminary experiments. A random integer number, between 1 and population size is determined as the cutting point and one-point crossover is applied. Since there are short chromosomes, one-point crossover was sufficient. The issue is modelled as a constrained problem of continuous optimization. The regression models given in Eqs (9) and (10) are used for this purpose, and then the GA algorithm is run under the given constraint via this model to optimize the factors Z function that is presented in Eq. (11) is the total error function and will be minimized by GA:

$$MinZ = \left|\left(Y_{1,target}/max(Y_{i1})\right) - \left(Y_{1,coded}/ maxYi1+Y2,target/maxYi2 - Y2,coded/maxYi2 \right. \quad \ldots (11)$$

$$\text{Min Z s.t.} X_1 \in [-1,1];\ X_2 \in [-1,1];\ X_3 \in [-1,1] \quad \ldots (12)$$

Note that the $Y_{1,target} = 1.75$ and $Y_{2,target} =$ 0.90in the equation of Z. In addition, $max(Y_{i1})$ and $max(Y_{i2})$ are the maximum observed response values presented in Table 3 (which are 1.809 and 0.906 for this problem, respectively). The CPU time is calculated as 25 seconds at a PC with a processor with Intel i5 2.4 GHz - 4 GB RAM. GA is calculated the optimized factor levels as $X_1 = 2.5$ (coded value: −1), $X_2 = 24.1624$ (coded value: −0.0406), and $X_3 = 41.2266$ (coded value: −0.7114). For this optimized factor level combination; the pole-body flux density and air-gap flux density are calculated as 1.7501 and 0.9061, respectively by continuous GA. When optimum factor levels are rounded to 1 decimal place according to mass production conditions ($X_1 = 2.5$, $X_2 = 24.2$, $X_3 = 41.2$), then the pole-body flux density and air-gap flux density are predicted by using Eq. (9) and Eq. (10) as 1.7512 and 0.9061, respectively.

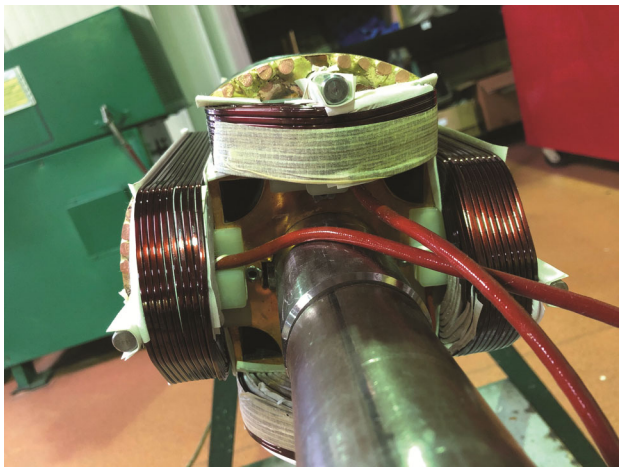

Fig. 6 — Manufactured rotor of the optimized SG

The maximum number of iterations for the PSO is selected as 1000 and the population size (swarm size) is selected as 100. Via a series of preliminary experiments, these PSO parameters were selected as follows: inertia weight (w) = 1, inertia weight damping ratio (w_{damp}) = 0.99, personal learning coefficient (C_1) = 1.5, and global learning coefficient (C_2) = 2.0. PSO is run through Eqs (9) – (12) and the optimized factor levels are calculated as $X_1 = 3.25$ (coded value: 0.5), $X_2 = 22.4648$ (coded value: −0.3838), and $X_3 = 41.2703$ (coded value: −0.7011).

For this optimized factor level combination; the pole-body flux density and air-gap flux densities are calculated as 1.75000098 and 0.9, respectively. The CPU time is calculated as 20.5 sec. When optimum factor levels are rounded to 1 decimal place according to mass production conditions (X_1 = 3.3, X_2= 22.5, X_3 = 41.3), then the pole-body flux density and air-gap flux density are predicted by using Eqs (9) & (10) as 1.749 and 0.8996, respectively.

The MSGO parameters are referred from the literature[22, 23] and via a series of preliminary experiments. The maximum number of iterations is selected as 1000 and the population size is selected as 30. MSGO is also run through Eqs (9) – (12) and the optimized factor levels are calculated as X_1 = 3.25 (coded value: 0.5), X_2 = 23.3784 (coded value: −0.1554), and X_3 = 41.2814 (coded value: −0.6985). For this optimized factor level combination; the pole-body flux density and air-gap flux density are calculated as 1.7499916 and 0.9, respectively. The CPU time is calculated as 15.22 sec. When optimum factor levels are rounded to 1 decimal place according to mass production conditions (X_1 = 3.3, X_2 = 23.4, X_3 = 41.3), then the pole-body flux density and air-gap flux density are predicted by using Eq. (9) and Eq. (10) as 1.7494 and 0.8996, respectively.

Optimization results of GA, PSO, and MSGO are also presented at Table 6. To confirm the optimization results, Maxwell simulations are performed. The overall prediction performances for all four methods are very good and PE (%) is less then %1. If the time complexity analysis is performed, it is clearly observed that RSM has advantages when compared with GA, PSO, and MSGO. CPU time is not applicable for RSM because it given the analysis results instantly. Also the original factor levels can be used instead of coding them. So coding and uncoding (after optimization) is not needed in RSM. Finally the better run parameters of GA and PSO is especially needed to be tuned before running; while RSM does not need any parameter optimization for gradient search. When the GA, PSO and MSGO are compared in each other, MSGO have less parameter to tune (only number of iterations and population size) which makes it very efficient as well.

When the optimum factor values obtained were also evaluated in terms of mass production, several remarkable inferences were obtained. For example, the results obtained show that as the Bs0 value approaches 3.5 mm, 3 enamel wire slots can pass through the opening width (Bs0) more easily and this width is more suitable for mass production. However, increasing this gap (Bs0) prevents reaching the desired magnetic flux values and efficiency in the stator. When the Bs0 value approaches the lower limit of 2.5, the magnetic flux and efficiency reach the desired level more easily, while 2 enamel wires can hardly fit into the slot opening width. This slows down the mass production considerably due to the enamel wires placed one by one in mass production. Accordingly, the most suitable value of Bs0 for mass production (also providing the desired magnetic density distribution value) was found to be 3.1.

In order for the salient pole of rotor to be magnetically saturated, the pole width of the rotor is expected to be as wide as possible. However, the winding to be wrapped around the salient pole can fit in a limited volume. Therefore, as the width narrows, the winding fits more easily into this predetermined limited volume (suitable for mass production); in the opposite direction (at which the optimum magnetic density distribution value can be obtained) the largest width was found to be 41.2 mm.

The results showed that pole height does not have a noticeable effect on responses for this sample SG structure in the article (causes little changes). The reason for this is efficient flux is occurred upper part of the pole. This causes the length of the pole height not to have much effect on the magnetic flux. As mentioned above, this issue is valid only for the SG considered in this case study.

These results and discussions can be expanded by using additional optimization methods such as hybridized improved GA[24], teaching learning based optimization[25], social group optimization (SGO)[26], jaya algorithm[27], non-dominated sorting SGO algorithm[28], and etc., in the future researches.

Conclusions

In this study rotor design optimization of 4-poled 1500 rpm 25 kVA SG is performed. The goal is to determine the optimal slot opening width (Bs0), height, and width factor levels to keep the magnetic flux density distribution in a desired range. The aim is to obtain 1.75 Tesla and 0.9 Tesla for the ‘pole-body flux density’ and ‘air-gap flux density’, respectively. RSM is used for optimization and the observations are obtained from Maxwell simulations. As a result, the desired magnetic flux distributions are obtained with a very small prediction errors (<0.05). R&D work was

successfully completed by obtaining 25 kVA from the SG as aimed in the tests carried out on the real prototype whose production was completed. Results obtained by RSM are also compared with GA, PSO and MSGO results. It is observed that although the results of the four methods are almost the same, however one of the advantages of RSM is that it does not require program coding and offers the opportunity to visually examine the relationships between factors and responses. According to the time complexity analysis, it is clearly observed that the RSM is less complex than GA, PSO, and MSGO. When the GA, PSO and MSGO are compared in each other, it can be clearly observed that MSGO have less parameter to tune and produces very accurate results which makes it very efficient as well. As a future research we will expand the work for higher power groups, additional design parameters, and additional optimization methods.

Acknowledgment

We would like to thank the Department of Research & Development at Isbir Electric Company for giving us the opportunity to use its facilities and applications. We would also like to thank Kemal Yilmaz and Mehmet Baki Dogru for their support. Finally, we thank for the supportive comments made by the editor and the anonymous reviewers that helped boost the coherence, accuracy, and reliability of this article.

References

1 Gizolme O, Thollon F, Clerc G & Rojat G, Shape optimization of synchronous machine rotor, *Int J Appl Electrom*, **9** (1998) 263–275.

2 Gillon F & Brochet P, Screening and response surface method applied to the numerical optimization of electromagnetic devices, *IEEE T Magn*, **36** (2000) 1163–1167.

3 Jolly L, Jabbar M A & Qinghua L, Design optimization of permanent magnet motors using response surface methodology and genetic algorithms, *IEEE T Magn,* **41** (2005) 3928–3930.

4 Fang L, Jung J W, Hong J P & Lee J H, Study on high-efficiency performance in interior permanent-magnet synchronous motor with double-layer PM design, *IEEE T Magn,* **44** (2008) 4393–4396.

5 Hasanien H M & Muyeen S M, A Taguchi approach for optimum design of proportional-integral controllers in cascaded control scheme, *IEEE Trans Power Syst,* **28** (2013) 1636–1644.

6 Zhang C J, Chen Z H, Mei Q X & Duan J J, Application of particle swarm optimization combined with response surface methodology to transverse flux permanent magnet motor optimization, *IEEE T Magn*, **53** (2017) Article Number: 8113107.

7 Chai W, Lipo T A, Kwon B I, Design and optimization of a novel wound field synchronous machine for torque performance enhancement, *Energies*, **11** (2018) article number: 2111.

8 Islam M J & Moghaddam, R R, Loss reduction in a salient pole synchronous machine due to magnetic slot wedge and semi-closed stator slots, in *13th Int Conf Electr Machines (ICEM) (*Alexandroupoli – Greece), 03–06 September 2018.

9 Soleimani J, Ejlali A & Moradkhani M, Transverse flux permanent magnet generator design and optimization using response surface methodology applied in direct drive variable speed wind turbine system, *Period Eng Nat Sci*, **7** (2019) 36–53.

10 Karaoglan A D, Ocaktan D G, Oral A & Perin D, Design optimization of magnetic flux distribution for PMG by using response surface methodology, *IEEE T Magn*, **56** (2020) 1–9.

11 Montgomery D C, *Design and analysis of experiments* (John Wiley & Sons, New Jersey–Haboken) 2013.

12 Mason R L, Gunst R F & Hess J L, *Statistical Design and Analysis of Experiments* (John Wiley & Sons, New Jersey–Haboken) 2003.

13 Karaoglan A D, Optimizing plastic extrusion process via grey wolf optimizer algorithm and regression analysis, *J Sci Ind Res*, **80** (2021) 34–41.

14 Thyssenkrupp Steel Europe, Non Grain oriented electrical steel powercore. [https://www.thyssenkrupp-steel.com/en/ (07 December 2020)]

15 Cetinceviz Y, Uygun D & Demirel H, Optimal design and verification of a PM synchronous generator for wind turbines, *Int J Renew Energy Res*, **7** (2017) 1324–1332.

16 Holland J H, *Adaptation in Natural and Artificial Systems* (MIT Press, Cambridge–UK) 1975.

17 Goldberg D E, *Genetic Algorithms in Search, Optimization and Machine Learning* (Addison-Wesley Longman Publishing Co. Inc., Boston, MA–USA) 1989.

18 Goldberg D E, *Genetic Algorithms in Search, Optimization and Machine Learning* (Addison-Wesley Longman Publishing Co. Inc., Boston, MA–USA) 1989.

19 Haupt R & Haupt S E, *Practical genetic algorithms* (John Wiley & Sons, New Jersey–Haboken) 2004.

20 Wei Y & Qiqiang L, Survey on particle swarm optimization algorithm, *Eng Sci*, **5** (2004) 87–94.

21 Robinson J & Rahmat-Samii Y, Particle swarm optimization in electromagnetics, *IEEE T Antenn Propag*, **52** (2004) 397–407.

22 Lalwani S, Sharma H, Satapathy S C, Deep K & Bansal J C, A survey on parallel particle swarm optimization algorithms, *Arab J Sci Eng*, **44** (2019) 2899–2923.

23 Naik A, Satapathy S C & Abraham A, Modified social group optimization-a meta-heuristic algorithm to solve short-term hydrothermal scheduling, *Appl Soft Comput*, **95** (2020) article number: 106524.

24 Naik A, Modified Social Group Optimizationalgorithm [https://www.mathworks.com/matlabcentral/fileexchange/78272-modified-social-group-optimization-algorithm (29 January 2021)]

25 Katari V, Satapathy S, Murthy J & Reddy P, Hybridized improved genetic algorithm with variable length chromosome for image clustering, *Int J Comput Sci Netw Secur*, **7** (2007) 121–131.

26 Rajinikanth V & Satapathy S C, Design of controller for automatic voltage regulator using teaching learning based optimization, *Proc Technol*, **21** (2015) 295–302.
27 Satapathy S & Naik A, Social group optimization (SGO): a new population evolutionary optimization technique, *Complex Intell Syst*, **2** (2016) 173–203.
28 Satapathy S C & Rajinikanth V, Jaya algorithm guided procedure to segment tumor from brain MRI, *Journal of Optimization*, **2018** (2018) Article Number: 3738049.
29 Satapathy S C, Naik A & Jena J J, Non-dominated sorting social group optimization algorithm for multi objective optimization, *J Sci Ind Res*, **80** (2021) 129–136.

GRAPHICAL ABSTRACT